13. Our analysis of flow results from superimposing an energy cone onto a computer image of the ground surface. The elevation and slope of the cone relative to the elevation and slope of the topography give the acceleration (deceleration), velocity, and runout time of the surge. The main parameters for motion parallel to ground surface are calculated from three equations:

$$a(i) = g(\sin \beta - \mu \cos \beta)$$

where $a(i)$ is the surge acceleration, g is the acceleration due to gravity, β is the slope of the land surface, and μ is the Heim coefficient (tangent of the energy line slope),

$$v^2(i) = v_0^2 + 2\, a(i)\, s(i)$$

where $v(i)$ is the velocity, v_0 is the initial velocity, and $s(i)$ is the slope distance, and

$$t(i) = 2\, s(i)/[v_0 + v(i)]$$

where $t(i)$ is the runout time. The results of this simple approach, schematically applied to the Mount St. Helens blast, are shown in Fig. 2. These values compare well with those observed [for example, see (*17*)]. The difference between the elevation of the energy surface and the ground topography, $\Delta h(i)$, directly yields the potential component velocity provided the surge is truly ground-hugging:

$$v(i) = [2g\Delta h(i)]^{1/2}$$

Taking boundary conditions into consideration, the total flow field vectors and streamlines and mass deposition per unit area can also be computed.
14. R. M. Batson, K. Edwards, E. M. Eliason, *J. U.S. Geol. Surv.* **3** (No. 4), 401 (1975).
15. B. Voight, *U.S. Geol. Surv. Prof. Pap. 1250* (1981), pp. 69–86.
16. S. W. Kieffer, *Nature (London)* **291**, 568 (1981); *U.S. Geol. Surv. Prof. Pap. 1250* (1981), pp. 379–400; R. P. Hoblitt, C. D. Miller, J. W. Vallance, *ibid.*, pp. 401–419; J. G. Moore and T. W. Sisson, *ibid.*, pp. 421–438; R. B. Waitt, Jr., *ibid.*, pp. 438–450.
17. C. J. Rice and D. K. Watson, *Eos* **62**, 557 (1981).
18. B. Voight, H. Glicken, R. J. Janda, P. M. Douglass, *U.S. Geol. Surv. Prof. Pap. 1250* (1981), pp. 347–377.

30 November 1981; revised 12 May 1982

Venus: Global Surface Radar Reflectivity

Abstract. *Observations of the surface of Venus, carried out by the Pioneer Venus radar mapper at a wavelength of 17 centimeters, reveal a global mean reflectivity at normal incidence of 0.13 ± 0.03. Over the surface, variations from a low of 0.03 ± 0.01 to a high of 0.4 ± 0.1 are found, with Theia Mons, previously identified as possibly volcanic, showing a value of 0.28 ± 0.07. Regions of high reflectivity may consist of rocks with substantial inclusions of highly conductive sulfides.*

The radar altimeter (*1*) carried aboard the Pioneer Venus Orbiter spacecraft is capable of determining three characteristics of that planet's surface: relief, roughness, and reflectivity. Results for the first two of these have been presented (*2, 3*); here we discuss some initial findings on reflectivity.

For small angles, θ, of departure from normal incidence to the mean resolved surface, a scattering law first derived by Hagfors (*4*) appears to provide a useful approximation to the observed echo strength. Over the range $0 \leq \theta \leq 10°$, to which altimeter observations are limited (*1*), this law may be written

$$\sigma_0(\theta) \simeq (\alpha^{-2}\rho/2)(\cos^4\theta + \alpha^{-2}\sin^2\theta)^{-3/2} \tag{1}$$

where σ_0 is the dimensionless specific radar cross section (actual radar cross section divided by associated surface area), ρ is the power reflectivity at normal incidence to a smooth surface, and α is the root-mean-square (r.m.s.) inclination (in radians) of coherently reflecting surface facets having dimensions larger than the observing wavelength (17 cm). We used the observed distribution of echo power in delay, converted to a distribution in the angle of incidence through the known observing geometry, to estimate the parameters ρ and α associated with each altimetric observation. Because of the restriction on θ, values of α larger than 0.17 (10°) are poorly determined.

Figure 1 represents the near-global smoothed distribution of reflectivity for the surface of Venus obtained from the radar altimeter over the period of its operation from 5 December 1978 through 18 March 1981. Comparable distributions of relief and of the slope parameter α (but for a smaller data set) are given in (*3*) as plate 1 and figure 4, respectively. The lateral resolution of the surface ("footprint") inherent in these measurements varies with spacecraft altitude as detailed in table 2 of (*3*), but has been smoothed to about 100 km in all the global maps.

The mean global reflectivity obtained from these observations (weighted by area) is 0.13 ± 0.03 (*5*), a result consistent with the far more restricted Earth-based radar observations (*6*). Excursions in reflectivity from a low of about 0.03 ± 0.01 to a high of 0.4 ± 0.1 are observed for the data shown in Fig. 1. These values have not yet been corrected for the possible presence of diffusely scattering material, which can reduce the surface area effective in the quasi-specular reflecting process below that calculated geometrically. To the extent such correction is required, the estimated reflectivity is increased. The amount of diffusely scattering surface material may be determined, at least approximately, from radar data taken at relatively high angles of incidence as well as from measurements of the depolarized echo component (*7*).

For a single surface layer, whose magnetic permeability is unity, the reflectivity is controlled solely by the complex dielectric discontinuity presented at the reflecting interface, and may be expressed as

$$\rho = |(1 - \epsilon^{1/2})/(1 + \epsilon^{1/2})|^2 \tag{2}$$

where $\epsilon = K + i[L + S/(\epsilon_0\omega)]$ is the complex dielectric constant of the bulk surface material. The real component, K, dominates the reflectivity for most dry terrestrial rocks and soils. The imaginary component depends in part on the dielectric loss, L, and in part on the volume conductivity, S, as well as on the permittivity of free space, ϵ_0, and the angular frequency of the incident radiation, ω. At radar frequencies ($\sim 10^9$ Hz), S must exceed about 0.1 mho/m to affect the reflectivity significantly; most dry terrestrial surface materials (except sulfide minerals) have S between 10^{-2} and 10^{-6} mho/m (*8*) and L of the order of 0.05 to 0.2 (*9*).

The bulk dielectric constant is controlled in part by the porosity and in part by the electrical properties of the constituents of the surface material. In general, for very porous or powdered material, K is low (typically 2.0 for a density of 1 g/cm^3) and largely independent of the type of material (*9*). For solid, dry terrestrial rocks at radar frequencies, on the other hand, K varies from about 5 for most granites up to as much as 9 for some basalts (*8*); for meteoritic material containing metallic and sulfide inclusions, the dielectric constant rises substantially above 9 (*9*).

To look for the extent to which the scatter in the observations might exceed the statistical fluctuations inherent in the data, we plotted each value of ρ in a given surface region against its conjugate value of α, both having been estimated simultaneously from a fit of Eq. 1 to the data of a given observation. The ensemble of points corresponding to the selected group of observations forms a scatter diagram and provides a useful way not only of confirming correlations between the estimated parameters but also of illustrating the internal consistency of the data set. The location of the centroid of the ensemble on the diagram categorizes the surface in terms of its gross radar scattering properties.

Figure 2 shows scatter diagrams drawn from the observational data for two selected areas of the surface. The first covers a major portion of Sedna Planitia and is fairly typical not only of the Venus lowlands but of most of the rolling uplands as well. The mean value of ρ for this region is 0.12 ± 0.03, corresponding to $K = 4.2 \pm 0.8$. The observed r.m.s. fluctuation about the mean (0.03) is consistent with the calculated formal error (typically about 0.03) of the individual values of ρ (*5*). The associated values of α, on the other hand, vary from about 0.8° to over 4°, a range larger than can be accounted for by the formal measurement error (typically about 0.5°) and thus indicative of a real variation in α over the (rather large) area considered, as suggested by figure 4 in (*3*). No significant correlation between the values of ρ and α is evident, although the formal correlation in the estimation of each parameter pair is typically about 0.75; presumably the correlation is lost because of the large spread in values of α intrinsic to this region. As mentioned earlier, the value of ρ estimated here may be slightly lower than the true value, perhaps by as much as 10 percent, because of the presence of diffusely scattering surface material. The lowest value of K for rocks commonly found on the earth's surface is about 5; thus the surface of Sedna Planitia may be nearly solid rock, although the measurements allow for the presence of a slightly porous regolith. For the lunar surface, which is known to be quite porous, K is observed to be about 2.7 (*6*). Note that the lowest value of ρ found on Venus, 0.03 (corresponding to $K = 2.0$), requires a material density of about 1 g/cm^3 (*9*) if reflection occurs at a single surface. Such a low density suggests porous material, perhaps unconsolidated sediment deposited by wind. Multilayer reflections are possible, of course, but a reasonable two-layer model developed by Hagfors (*4*) cannot yield a net reflectivity as low as 0.03 if the upper layer overlies material with average Venus surface properties at a depth capable of interacting significantly with the radar waves.

The second scatter diagram (Fig. 2b) shows the results of 24 observations grouped over Theia Mons, the more southerly of the two mountains in the Beta Regio and a feature thought to be volcanic in origin (*10*). Figures 1 and 2b show that the reflectivity of this region is substantially higher than is typical for the rest of the surface. The r.m.s. slope is also higher, but well below the 10° limit for accurate determination. The r.m.s. scatter (0.05 in ρ, 1.7° in α) of the points around their mean (whose coordinates are $\rho = 0.28 \pm 0.07$, $\alpha = 5.3° \pm 1°$) is reasonably consistent with the typical formal errors (0.06 in ρ, 1° in α) of individual points. Some correlation is evident but less than the formal value of 0.92, suggesting intrinsic variability in this area as well. The value of K corre-

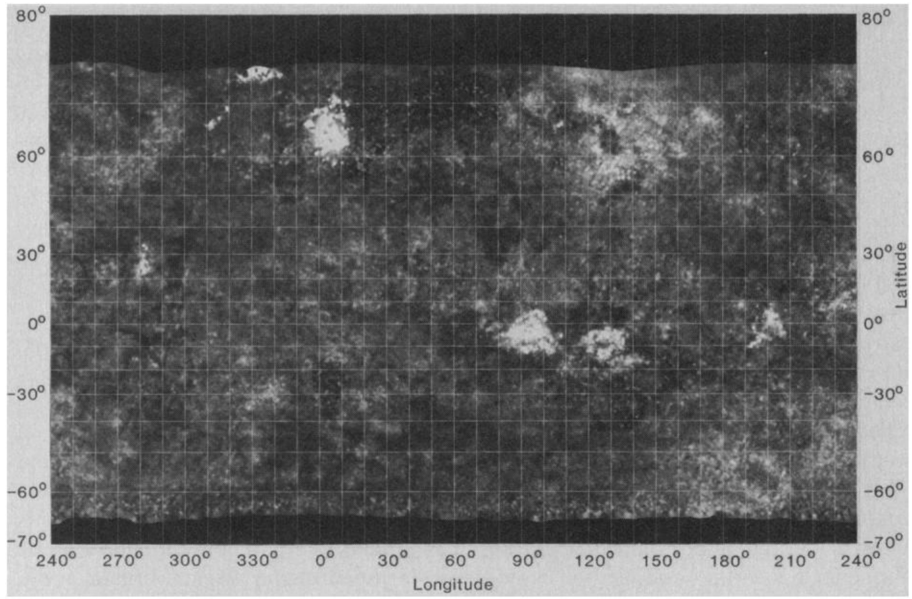

Fig. 1. Global map of the variation in the power reflection coefficient of the surface of Venus obtained at a wavelength of 17 cm by the Pioneer Venus radar altimeter. The brightest areas have reflectivities of 0.25 or more, while the darkest correspond to 0.05 or less. The large bright areas centered at 65°N,5°E and 5°S,95°E correspond to the Maxwell Montes and elevated regions of Terra Aphrodite, respectively. Also bright and elevated is a relatively small region surrounding Theia Mons at 24°N,281°E, a feature that may be volcanic (*10*).

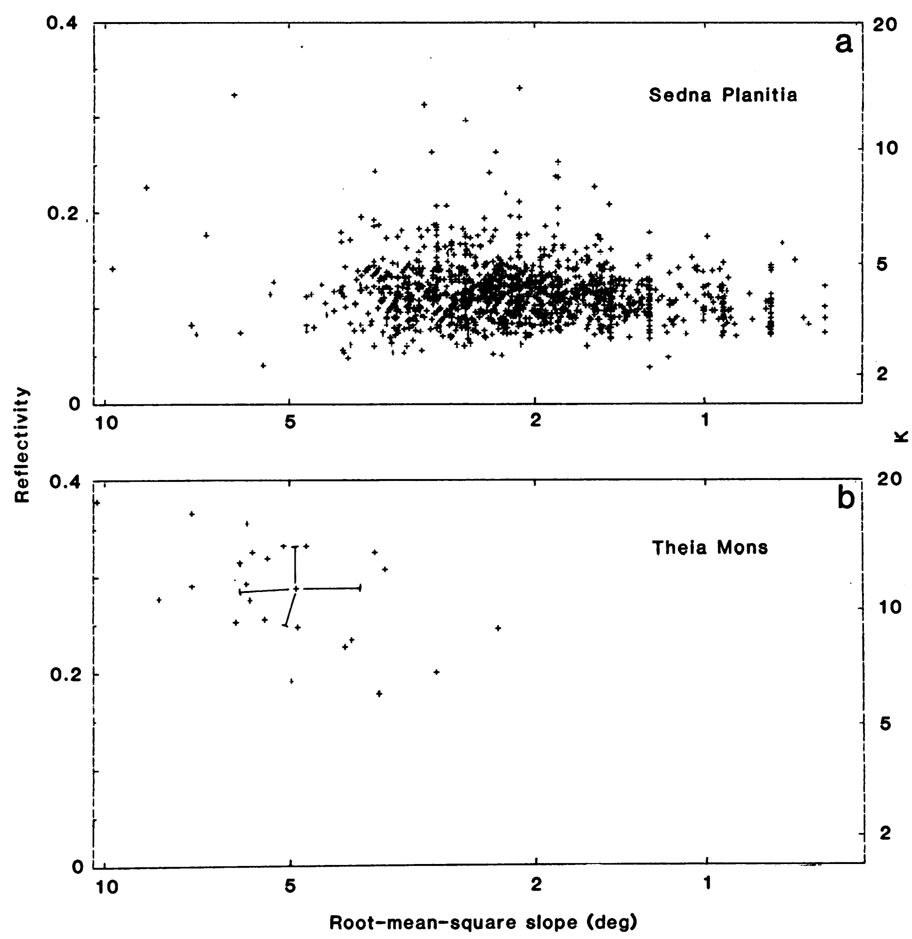

Fig. 2. Scatter diagrams showing the dispersions of reflectivity (ρ) and r.m.s. slope (α) for data from selected regions of the Venus surface. (a) Sedna Planitia: 30° to 45°N, 310° to 360°E; (b) Theia Mons: 22° to 26°N, 279° to 282°E. The real part of the dielectric constant, K, shown on the right ordinate, was calculated from Eq. 2, assuming that the conductivity and loss are negligible. Clumping of data around "preferred" values of r.m.s. slope, predominately below 1.5°, is an artifact of the data analysis and reflects a resolution limit in the radar system.

sponding to the average reflectivity is 11 ± 4, a moderately high value for a dry planetary surface at radar frequencies. For other parts of Venus where the reflectivity approaches 0.4, K calculated by assuming negligible conductivity and loss rises to 20.

How can these relatively high reflectivities be explained? From Eq. 2 we see that both the real and imaginary parts of ϵ contribute to the reflectivity. It seems extremely unlikely that dielectric losses (L) of naturally occurring dry rocks could be large enough to dominate the reflection mechanism; they normally control only the attenuation with depth (*9*). For the conductivity, S, to be important in reflection, not only must it exceed about 0.1 mho/m at our radar's operating frequency, but the conductive region must extend over an area with dimensions comparable to a wavelength or larger. If such large areas of conductive surface exist, it would seem likely that, at least occasionally, reflectivities near unity would be encountered, since occurrence of the precise frequency-dependent threshold value of S necessary to yield reflectivities consistently between 0.3 and 0.4 seems highly fortuitous.

We are left, then, with the necessity for explaining how the real part, K, of the dielectric constant can be raised to values between 11 and 20. The most likely mechanism is the presence in the rock of conducting inclusions much smaller than the observing wavelength. Meteorites containing relatively large amounts of free iron-nickel mixtures and sulfides display values of K ranging up to 100 or more (*9*). Free metals seem unlikely and in any case could not exist for long in any part of the Venus surface exposed to the atmosphere; highly conducting metallic sulfides would also be unstable to atmospheric exposure (*11*). But if overturning of the first few centimeters of surface proceeds slowly enough, or if material is being steadily stripped off the surface and blown elsewhere, atmospherically unstable minerals could be maintained sufficiently near the surface to be effective in raising the dielectric constant.

Nozette and Lewis (*12*) suggested that chemical erosion takes place at high elevations on Venus, where winds are comparatively strong and atmospheric densities and temperatures relatively low. The fine-grained eroded material is subsequently delivered to lower elevations, where it is chemically modified and possibly compacted. In the process, the putative conducting inclusions are transformed into gases and nonconducting minerals. If the "original" Venus surface contained on the order of 15 percent free metal—or, more likely, pyrite (FeS_2), which has been postulated independent of radar observations to explain the observed atmospheric chemical composition (*11*)—the high values of reflectivity seen at high elevations could be readily explained. Pyrite is one of very few minerals with the necessary high conductivity, having values between 1 and 10^5 mho/m (*8*).

The model that emerges from this discussion requires that the surface of Venus in the vicinity of the highly reflecting regions contain a significant amount of conducting mineral as inclusions in the rock. From a consideration of the present lower atmospheric composition, this material is likely to be pyrite and may be widespread in the original crustal rock, lying in radar view only at higher elevations, where new surface is constantly being exposed. It is also possible that pyrite is preferentially produced in sulfur-rich volcanic material.

G. H. PETTENGILL
P. G. FORD
S. NOZETTE
Department of Earth and Planetary Sciences, Massachusetts Institute of Technology, Cambridge 02139

References and Notes

1. G. H. Pettengill, D. F. Horwood, C. H. Keller, *IEEE Trans. Geosci. Remote Sensing* **GE-18**, 28 (1980).
2. G. H. Pettengill, P. G. Ford, W. E. Brown, W. M. Kaula, H. Masursky, E. Eliason, G. E. McGill, *Science* **205**, 91 (1979); H. Masursky, E. Eliason, P. G. Ford, G. E. McGill, G. H. Pettengill, G. G. Schaber, G. Schubert, *J. Geophys. Res.* **85**, 8232 (1980).
3. G. H. Pettengill, E. Eliason, P. G. Ford, G. B. Loriot, H. Masursky, G. E. McGill, *J. Geophys. Res.* **85**, 8261 (1980).
4. T. Hagfors, *Radio Sci.* **5**, 189 (1970).
5. Errors in the estimates derived from the observational data are of two kinds: (i) a formal standard error resulting from the weighted-squares estimation, which is dependent both on the analytic form of the scattering model and on the fluctuation noise associated with the data. These standard errors vary, but for ρ and α typically range between 10 and 30 percent of the estimated value of the associated parameter. As a large number of results for a geographic region are averaged, however, the uncertainty in the mean from this source rapidly diminishes until (ii) the residual systematic error comes to dominate. The systematic error reflects failures in the accuracy of the modeling and, for ρ, uncertainties in the radar system calibration. Many of the systematic effects are common to large groups of the observations and are difficult to estimate. We have, somewhat arbitrarily and, we hope, conservatively, placed our estimates of the upper limit to systematic uncertainty here at about 25 percent of the associated value. The errors on all the numerical results in this report reflect primarily the absolute systematic uncertainties; comparisons among our results may therefore carry more precision than is apparent, since the corresponding errors are largely systematic.
6. G. H. Pettengill, *Annu. Rev. Astron. Astrophys.* **16**, 265 (1978).
7. ——— and T. W. Thompson, *Icarus* **8**, 457 (1968).
8. G. V. Keller, In *Handbook of Physical Constants*, S. P. Clarke, Jr., Ed. (Geological Society of America, New York, 1966), p. 553.
9. M. J. Campbell and J. Ulrichs, *J. Geophys. Res.* **74**, 5867 (1969).
10. R. S. Saunders and M. C. Malin, *Geophys. Res. Lett.* **4**, 547 (1977).
11. U. von Zahn, S. Kumar, H. Niemann, R. Prinn, in *Venus*, D. Hunten and L. Colin, Eds. (Univ. of Arizona Press, Tucson, in press).
12. S. Nozette and J. S. Lewis, *Science* **216**, 181 (1982).
13. We are grateful to E. Eliason for assistance in preparing Fig. 1 and to R. Prinn for pointing out the potentially significant role of FeS_2 in the surface and atmospheric chemistry of Venus. This research has been supported by a contract with the NASA Ames Research Center.

27 January 1982; revised 8 June 1982

Cigarette Smoke Contains Anticoagulants Against Fibrin Aggregation and Factor XIIIa in Plasma

Abstract. *Gas-phase, water-soluble components of cigarette smoke cause delayed fibrin self-assembly and prevent fibrin cross-linking by inactivation of factor XIIIa (plasma transglutaminase). These anticoagulant properties of smoke are demonstrable in plasma, suggesting they play a role in the pathophysiology of smoking.*

There is little information on the effects of cigarette smoke on important biochemical interactions, though considerable information on its physiologic effects is available. Studies on interactions of cigarette smoke with certain proteins have provided biochemical evidence that specific functions of such proteins are inhibited (*1, 2*) or augmented (*3*) by smoke components. In view of the shortened half-life of radioactively labeled fibrinogen in dogs exposed to cigarette smoke (*4*) and of the reported increase in fibrinogen in human smokers (*5*), we examined the possible effect of smoke on certain fibrinogen functions in vitro. We found that water-soluble smoke components include two types of anticoagulants: one is directed against fibrin self-assembly and the other inactivates factor XIIIa, thereby preventing cross-link formation (that is, stabilization) in fibrin clots.

Fibrinogen, a plasma glycoprotein, consists of three pairs of disulfide-bridged polypeptide chains termed Aα (molecular weight, ~ 70,000), Bβ (~ 60,000), and γ (~ 50,000). Cleavage by thrombin of arginyl-glycine peptide bonds at positions Aα16 and Bβ14 results in release of small polar peptides A and B from their respective chains: the resulting fibrin monomers polymerize noncovalently and form the fibrin gel.

